

# Reliability studies on integrated GaAs power-sensor structures using pulsed electrical stress

C. Sydlo, K. Mutamba, L. Divac Krnic<sup>a</sup>, B. Mottet and H.L. Hartnagel

*Inst. für Hochfrequenztechnik, TU-Darmstadt, Merckstr. 25, D-64283 Darmstadt, Germany*

*E-mail: c.sydlo@ieee.org, Tel.: +49 6151 16 2662, Fax: +49 6151 16 4367*

*<sup>a</sup> Multimedia Communications Lab, TU-Darmstadt, Merckstr. 25, D-64283 Darmstadt, Germany*

---

## Abstract

The transmission line pulse method (TLP) is used to characterise the reliability of bolometric GaAs microwave power-sensors. Two degradation mechanisms are identified during the degradation process of the absorbing NiCr termination, in which the input power is converted into heat. Simulations and a material analysis have been performed in order to characterise the observed degradation mechanisms.

---

## 1. Introduction

This paper reports on the reliability study of thermoelectrical GaAs power sensors using the transmission-line pulse method (TLP) [1,2]. For this type of micromachined sensor, which is based on a bolometric principle, a proper termination is of critical importance for its performance. A higher sensitivities and linearities can be achieved through a (proper) matching as well as (proper) choice of resistor material with minimum temperature coefficient. For the commercial viability of such a sensor through reliability studies, concerning material as well as the corresponding geometry are of great importance as they guarantee an optimal integration of the device in existing circuits and systems [3]. The particular technology, used in this work, is MMIC compatible and can be adapted to standard GaAs based processes.

A first analysis is made for millimeter-wave power sensors, as shown in figure 1, followed by a systematic approach with corresponding test structures. These test structures have been defined as resistive terminations of different geometries on GaAs substrate.

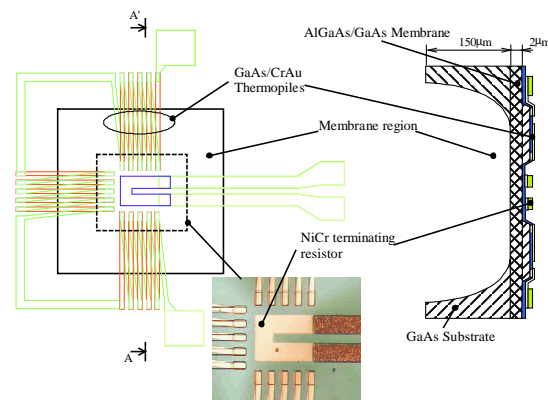


Figure 1: Sensor layout and cross-section of the membrane structure for the thermal isolation. The photograph shows the NiCr termination as well as the hot ends of the thermopiles in the center of the membrane.

The main degradation mechanism has been identified to be a current-induced metal migration at

regions of high current densities followed by a field-induced material transport in the damaged regions. Simulations as well as material analysis after failure support this classification.

## 2. Device description

The sensor structure includes coplanar striplines terminated by a NiCr(80/20) resistor, in which the microwave power is converted into heat. The micromachined AlGaAs membrane area provides a thermal insulation from the rest of the bulk. The temperature difference is measured using GaAs/CrAu thermopile systems. The output thermo-voltage is proportional to the effective value of the microwave power. The sensitivity of 11 V/W is constant over the frequency range up to 80 GHz [4,5].

Additional test structures are defined to optimise the power handling capability of the device. Therefore, different geometries of the NiCr resistive layer, used in the sensor, have been chosen in order to achieve an uniform current distribution in the termination.

## 3. Experimental set-up

The computer-controlled measurement set-up mainly consists of a parameter analyser (HP4145A), a pulse generator (HP8114A), an oscilloscope (TDS620) for pulse response monitoring and a switching matrix. Additional probe-heads have been designed and realised for this purpose. A microscope camera takes a picture after each stress cycle. All components are computer-controlled and allow a fully automated testing procedure. Software has been written to allow high flexibility in stress and measurement cycles. This set-up allows device-specific stress and analysis procedures for the identification of degradation mechanisms with any metallization.

## 4. Detection of degradation threshold

The threshold detection measurement is performed on resistors of different geometries as described in table 1 and inset of figure 2, using electrical pulses with a length of 100 ns. The influence of the chosen geometry on the device power handling capabilities is determined by varying the amplitude of the pulses applied to the device under test. Degradation is detected by the subsequent IV-measurements of the devices after a stress cycle. A rise in resistivity is

observed when degradation occurs.

Below the respective threshold voltages, no change of the resistances could be observed, even with an increase of the pulse numbers.

Table 1

Geometry description of investigated resistor structures. Angle and gap are indicated in figure 2.

Device	Angle /deg	Gap / $\mu\text{m}$
1.1	180	60
1.2	90	60
1.3	60	60
2.1	180	20
2.2	30	20
2.3	140	20
2.4	60	20
2.5	90	20

As shown in the measurement results in figure 2, a lower degradation threshold is observed on the samples with lower included angle. This threshold reduction can be explained by the current density increase in the corner region [6,7].

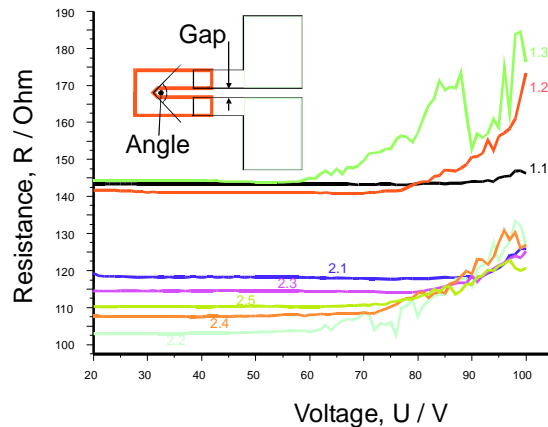


Figure 2: Change of resistances as a function of the applied electrical stress. Structures with sharp included angles show a lower degradation threshold.

Simulations have been performed for a characterisation of the degradation mechanisms and the extraction of the current densities in the NiCr-resistors (figure 3). The different geometries have been modelled and calculated with a FEM software [8]. The rise in current density within the region of the included angles is the source of the initial degradation and has therefore been taken as a figure of merit.

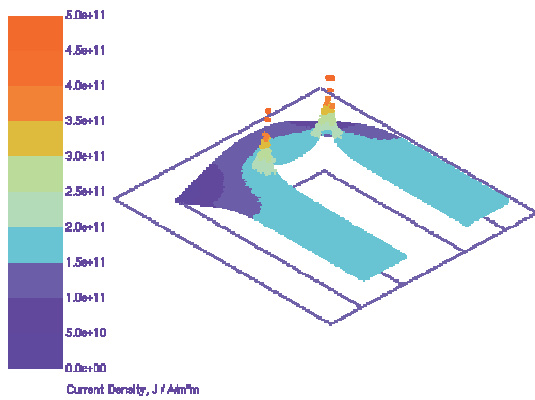


Figure 3: Numerical calculated current density distribution within the NiCr metallization (device 1.1). Single mesh cells are coloured and elevated by their current density.

The CDIF parameter (current density increase factor) has been introduced in order to evaluate the current densities in the corners in dependence of the applied stress. The obtained linearity between the  $1/CDIF$  and the observed degradation threshold current, as shown in figure 4, is a clear indication for a current density induced failure mechanism. Thermal failure, on the contrary, would result in a quadratic dependence.

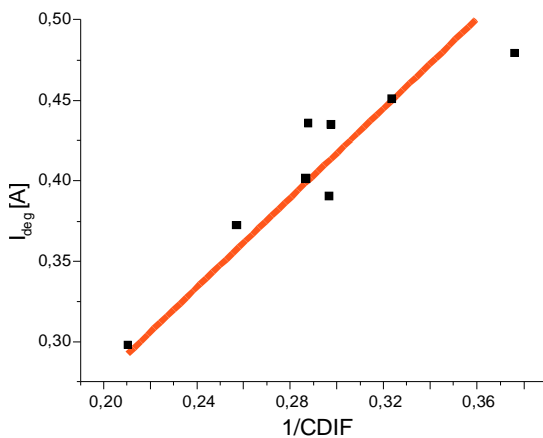


Figure 4: Linear relation between  $1/CDIF$  (current density increase factor) and the observed degradation threshold current.

For this failure mechanism the product of  $CDIF$  and the degradation threshold current is a constant

number for the used material system. Thus, enabling to estimate the degradation threshold current for any other resistor geometry during the design phase of the sensor structure.

## 5. Failure mechanism investigations

Using the TLP method, the main device failure mechanism has been identified to be the degradation of the NiCr termination resistor with increasing input power.

Initially, the degradation occurs in the regions with the highest current density (figure 5.2-5.4) and therefore highest thermal excitation. This leads to a current induced metal migration of the NiCr resistor metal and a damage to the underlying GaAs surface. The observed material transport is facilitated by the combined effect of local high temperatures and high current densities. With progressing degradation the resistance locally increases and therefore leads to high electric fields in the already damaged regions (figures 5.5-5.9). As a result, a second material transport mechanism is observed, which includes now also the non-passivated GaAs surface. Sub-picture 8 and 9 in figure 5 show small particles close to the burned areas indicating a transport of material away from the damaged regions of the NiCr resistor.

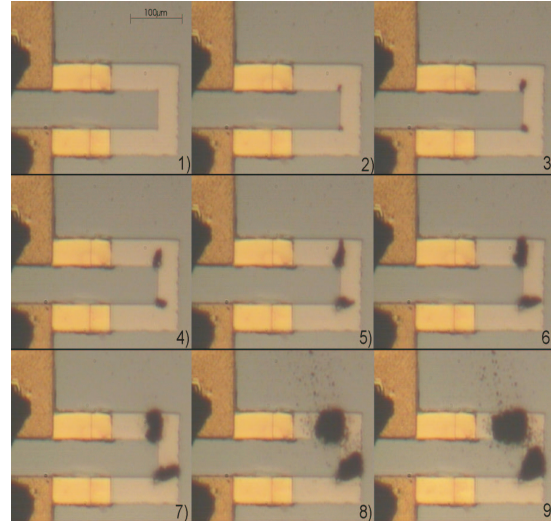


Figure 5: Degradation process in the NiCr test resistor. Current induced effects as appearing in subpictures 2-4 are followed by field induced effects from subpicture 5 on (device 1.1).

Figure 6 shows the removal of GaAs substrate material below the metallization and in the gap of the resistor. The initial current-induced degradation region (CIDR) is located in the upper left corner of figure 6 (right), whereas the field-induced degradation region (FIDR) lies in the gap between the lines.

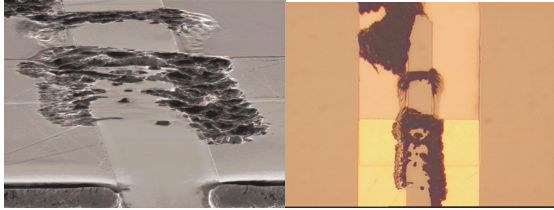


Figure 6: Surface damage and field induced material transport after cleaning the sample (device 2.5).

This description of the degradation process is supported by the before mentioned numerical modelling of the current densities and electric fields as well as material analyses based on energy dispersive x-ray (EDX). The latter method, which was used immediately after degradation, allows to show the composition of the transported material, which includes mainly GaAs from the substrate and a lower amount of the used metallization materials as shown in figure 7. The relatively high Cr content compared to Ni is due to presence of Cr as an adhesion layer for Au metallization.

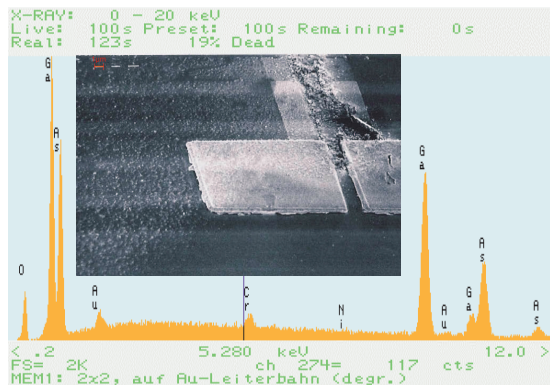


Figure 7: Energy dispersive x-ray analysis of the material transport in the degraded structure before cleaning (device 2.5).

## 6. Conclusion

The pulsed approach for the excitation of degradation mechanisms has been used to study the reliability of a power sensor structure. The main advantage of the degradation analysis is the possibility to stop the degradation process at any stage for sufficient measurements and analysis. This work shows the importance of the chosen approach for the improvement of sensor design and technology.

For this type of resistance structures the current induced degradation mechanisms trigger the field induced ones by producing a pre-damage into the structure of the underlying substrate material. Without such a pre-damage a pure field induced degradation is not observed.

## References

- [1] M. Brandt et al., Characterization of reliability of compound semiconductor devices using electrical pulses, *Micoelectron. Reliab.*, Vol. 36, No. 11/12, pp. 1991-1894, 1996.
- [2] D. C. Wunsch, R. R. Bell: Determination of Threshold Failure Levels of Semiconductor Diodes and Transistors due to Pulse. *IEEE Trans. Nuc.Sci.*, No.17, Dec. 1970
- [3] H.L. Hartnagel, A. Megej and K. Mutamba, Microwave and millimeter-wave monolithic signal source with MEMS-based power monitoring for sensing applications, Abstract book Office of Naval Research Workshop on Physical Effects and Device/Circuit Interactions in Solid State Devices, Bar Harbor, Main, USA, Sept. 2001.
- [4] Kabula Mutamba, Klaus Beilenhoff, Alexander Megej, Claus Woelk and Hans L. Hartnagel *Micromachined GaAs Sensors for Microwave and Millimeter-Wave Power Measurement*, MSTNEWS, No. 2/01, pp. 42-43, 2001.
- [5] A. Dehe, V. Krozer, B. Chen and H.L. Hartnagel, High-sensitivity microwave power sensor for GaAs-MMIC implementation, *Electronic Letters*, Vol. 32, No. 20, pp. 2149-2150, 1996.
- [6] J. R Black : *Electromigration Failure Models in*

Aluminum Metallization for Semiconductor Devices,"  
Proc. of the IEEE, vol. 57, no. 9, pp. 1587-1594,  
1969.

[7] Karl-Heinz Kretschmer, Die laterale  
Materialwanderung zwischen Elektroden und ihr  
Einfluss auf die Zuverlässigkeit planarer GaAs-  
Bauelemente, PhD Thesis, TU Darmstadt, 1987

[8] C. Geuzaine, P. Dular and J-F. Remacle, General  
Environment for the treatment of discrete problems,  
website: [www.geuz.org](http://www.geuz.org)